JACS
JOURNAL OF THE AMERICAN CHEMICAL SOCIETY
pubs.acs.org/JACS
Article

Probing Heterogeneous Charge Distributions at the α-Al_2O_3(0001)/H_2O Interface

Stefan M. Piontek, Mark DelloStritto, Bijoya Mandal, Tim Marshall, Michael L. Klein, and Eric Borguet*

Cite This: J. Am. Chem. Soc. 2020, 142, 12096−12105
Read Online
ACCESS | Metrics & More | Article Recommendations | Supporting Information

ABSTRACT: Unlike metal or semiconductor electrodes, the surface charge resulting from the protonation or deprotonation of insulating mineral oxides is highly localized and heterogeneous in nature. In this work the Stark active C≡N stretch of potassium thiocyanate is used as a molecular probe of the heterogeneity of the interfacial electrostatic potential at the α-Al_2O_3(0001)/H_2O interface. Vibrational sum frequency generation (vSFG) measurements performed in the OH stretching region suggest that thiocyanate species organize interfacial water similarly to halide ions. Changes in the electrostatic potential are then tracked via Stark shifts of the vibrational frequency of the thiocyanate stretch. Our vSFG measurements show that we can simultaneously measure the vSFG response of SCN^- ions experiencing charged and neutral surface sites. We assign local potentials of +308 and −154 mV to positively and negatively charged aluminol groups that are present at pH = 4 and pH = 10, respectively. Thiocyanate anions at positively charged surface sites and negatively charged surface sites and those participating in contact ion pairing adopt similar orientations and are oppositely oriented relative to thiocyanate ions near neutral surface sites. All four species followed Langmuir adsorption isotherms. Density functional theory−molecular dynamics (DFT-MD) simulations of SCN^- near the neutral α-Al_2O_3(0001)/H_2O interface show that the vSFG response in the C≡N stretch region originates from a SCN−H−O−Al complex, suggesting the surface site specificity of these experiments. To our knowledge this is the first spectroscopic measurement of local potentials associated with a heterogeneously charged surface. The ability to probe the evolution of local charges in situ could provide vital insight into many industrial, electrochemical, and geochemically relevant interfaces.

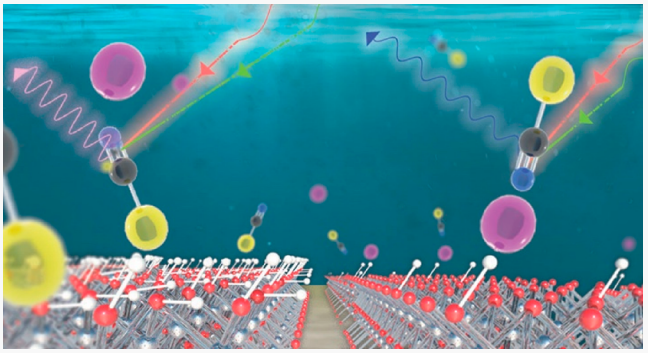

INTRODUCTION

The structure of water at interfaces plays an important role in many chemical, biological, and environmental processes.[1] Previous work has demonstrated that interfacial water structure at both charged and neutral interfaces can differ greatly compared to the bulk.[2] The presence of an interface can change the properties of the solvent, such as vibrational energy-transfer rates, hydrogen-bonding strength, and structure of the hydrogen-bonding network.[3,4] Mineral oxides are covered with surface hydroxyl groups, e.g., α-Al_2O_3(0001) (~15 OH groups/nm^2),[5,6] and thus allow for access to neutral, positive, and negative solid/H_2O interfaces through modulation of the bulk pH.[7] Deprotonation of surface aluminol groups creates a negatively charged surface at pH > 8, and protonation results in a positively charged surface at pH < 6, yielding a point of zero charge (PZC) range of ~6−8.[8,9] Furthermore, the insulating nature of alumina gives rise to local surface charges and a heterogeneous charge distribution at the surface.[7]

One of the driving forces in the reorganization of interfacial water is the surface charge. Water molecules orient themselves to minimize their free energy with respect to local charges,[10] and this reorganization of interfacial molecules can change the free energy of adsorption for solutes, affecting interfacial chemistry, e.g., heterogeneous catalysis.[11,12] The interfacial electric fields generated via photoexcitation or applied potentials can affect rate-determining steps in heterogeneous catalysis,[13] electrochemistry,[14] solar-energy generation,[15,16] and layered-material synthesis.[17] Thus, it is paramount that we have a detailed understanding of the local structure of polar solvents at charged surfaces.

The reorganization of interfacial water induced by surface charging has been characterized using vibrational sum frequency generation (vSFG), a surface-specific vibrational spectroscopy, at a variety of oxide/water interfaces: SiO_2/H_2O,[18] quartz/H_2O,[19] hydrophobic/H_2O,[20] TiO_2/H_2O,[21] and

Received: February 4, 2020
Published: July 6, 2020

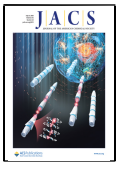

https://dx.doi.org/10.1021/jacs.0c01366
J. Am. Chem. Soc. 2020, 142, 12096−12105

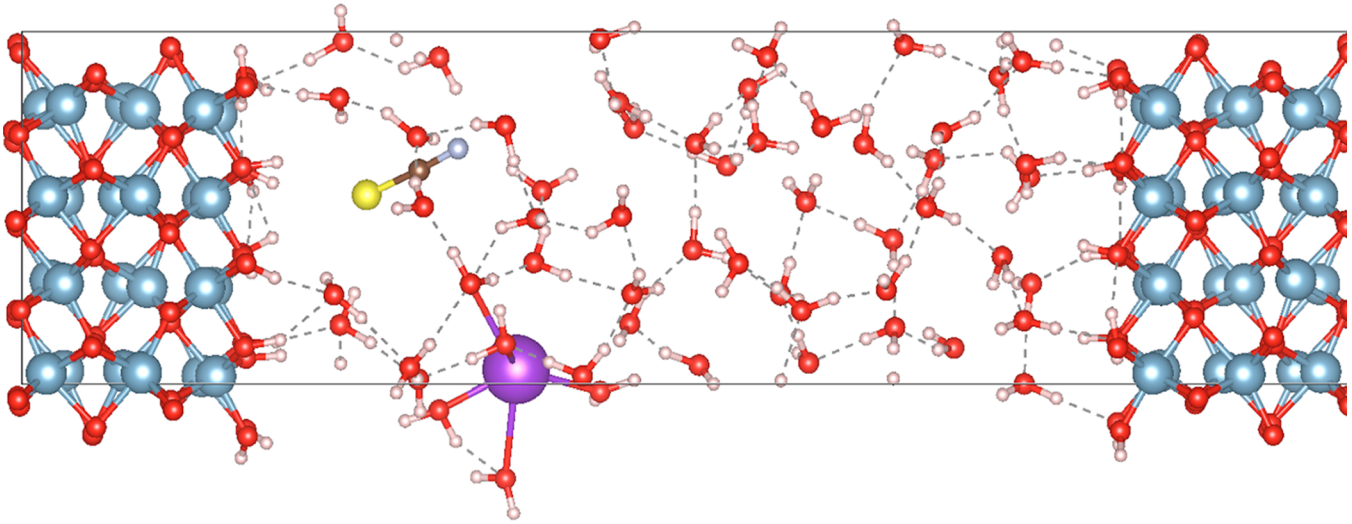

Figure 1. Snapshot of the α-$Al_2O_3(0001)/H_2O$ interface with KSCN as the molecular probe generated from our DFT-MD simulations. Here the red, white, light blue, gray−blue, brown, yellow, and purple atoms are O, H, Al, N, C, S, and K, respectively.

α-Al_2O_3/H_2O.[4,9] While these experiments can indirectly track charge accumulation via the interfacial solvent response, direct spectroscopic measurements of the surface charges at buried solid/liquid interfaces have remained elusive. vSFG allows us to probe molecular vibrations located at the solid/liquid interface because it is an inherently surface-specific technique within the dipole approximation.[19,22] To investigate the interfacial hydrogen-bonding environment using vSFG, a narrowband visible pulse is combined with a broadband IR pulse resonant with the O−H stretching vibrations. This allows for surface-specific vibrational spectroscopy of surface hydroxyls and water molecules in the interfacial region. vSFG is limited when it comes to studying surface charge, however, as many different sources of surface charge including protonation/deprotonation of surface groups,[3] specific adsorption of ions,[2,23] and variation of diffuse layer thickness can all give rise to similar changes in the intensity and shape of the spectrum.[24] Additional information is required to obtain a detailed picture of the surface structure and charge distribution at oxide surfaces, which are crucial parameters in understanding geochemically relevant buried interfaces.[25]

Vibrational Stark effect spectroscopy (VSES) correlates the shifts in vibrational frequencies of functional groups, e.g., nitrile, azide, and carbonyl bonds, to changes in the local electrostatic potential, thereby providing a method to measure the strength of local electric fields.[26−30] Second harmonic generation (SHG) has also been used to measure average interfacial potentials, although it lacks the ability to resolve the distinct local potentials associated with different sites.[31,32] VSES has been used to study how local electric fields aid in enzymatic function by inserting Stark active molecular probes into proteins.[33−36] VSES has also been used to investigate charge accumulation at electrochemical interfaces via the Stark shift of ionic liquids[37] and electrolyte solutions[38] and to probe molecules embedded in chemically bound self-assembled monolayers (SAMs) at electrochemical interfaces.[39−41] The frequency of the C≡N stretch is sensitive to the nature of the local environment, making SCN^- an excellent example of a Stark active molecule. Bulk IR spectra of KSCN have reported the SCN^- stretch at 2056 cm^{-1} in D_2O solutions,[42] 2057 cm^{-1} in methoxyethanol,[43] and ∼2050/2067 cm^{-1} for the free SCN^- and contact ion pairs of K^+ SCN^- in glassy liquids.[44] Recent vSFG studies have employed self-assembled monolayers (SAMs) containing Stark active molecules chemically bound to working electrodes to track changes in the local potential during surface charging and chemical binding.[45−48] The nitrile stretch frequencies in these studies have been reported at ∼2128 and ∼2100 cm^{-1} for chemically bound[47] and unbound[38] SCN^-, respectively. While these experiments yield information about the interfacial electrostatic potential, they require chemical modification of the surface and a conductive metal substrate. Furthermore, the potential measured corresponds to the average charge density, which is homogeneously distributed across the working surface, quite different from the heterogeneous sites (charged and neutral) at an insulating mineral oxide surface such as α-$Al_2O_3(0001)$.

Unlike metals and semiconductors, characterized by uniformly distributed surface charge, protonation and deprotonation of the terminal aluminol groups on the α-$Al_2O_3(0001)$ surface leads to highly localized charges on the interface.[49] The determination of the point of zero charge (PZC) and isoelectric point (IEP) of various alumina oxide surfaces remains controversial, with factors such as the exposed plane,[50,51] sample manufacturer,[7] crystal miscut,[7] choice of electrolyte,[7] and sample preparation affecting the observed PZC obtained from streaming potential measurements.[52] Many of these controversies arise from the inability to access surface aluminol groups directly. SHG[31] and vSFG[9] experiments at the α-$Al_2O_3(0001)/H_2O$ interface have explained the bulk pH dependence of the nonlinear response with reference to macroscopically determined surface acid dissociation constants (pK_a's) of γ-Al_2O_3.[53] However, γ-Al_2O_3 is less stable than α-Al_2O_3 and is described by a cubic unit cell, whereas α-Al_2O_3 is composed of hexagonal unit cells. We believe that previous authors have used γ-Al_2O_3 to describe the acid/base dissociation rates of α-$Al_2O_3(0001)$, because the pK_a's of the α-$Al_2O_3(0001)$ surface have never been measured directly, highlighting the difficulty of accessing the nature of surface aluminol groups. Clearly the surface preparation, as well as the corresponding variation in the molecular architecture of mineral oxides, leads to a wide range of macroscopic surface properties. This is illustrated by the variation in reported PZCs

https://dx.doi.org/10.1021/jacs.0c01366
J. Am. Chem. Soc. 2020, 142, 12096−12105

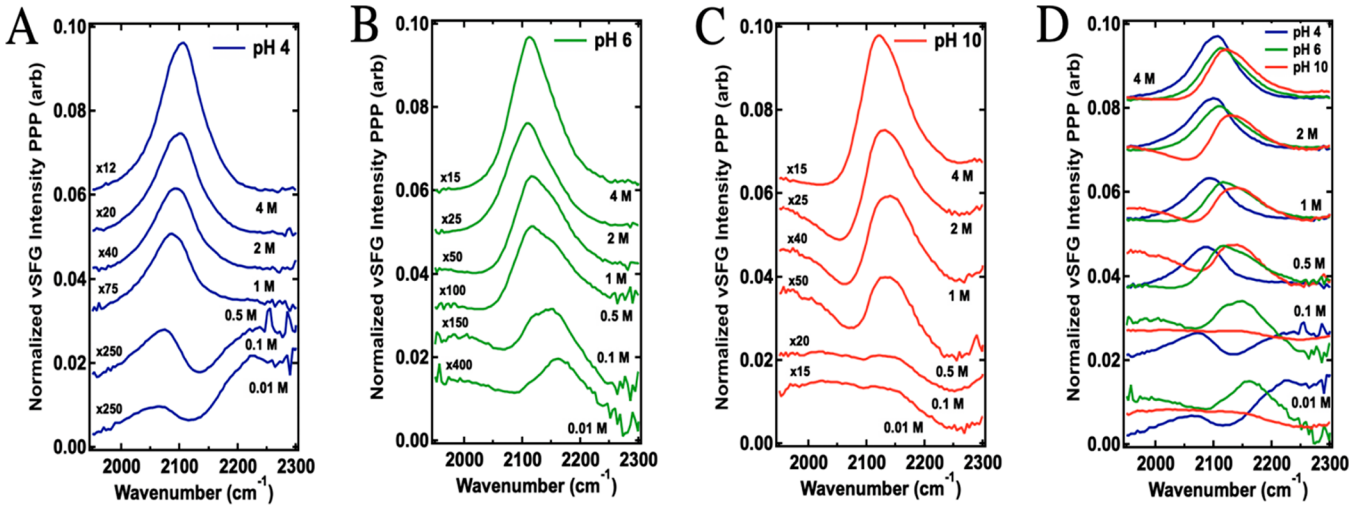

Figure 2. vSFG spectra of 1×10^{-2} to 4 M KSCN solutions at the α-$Al_2O_3(0001)$/aqueous interface for bulk pH = (A) 4, (B) 6, and (C) 10. The vSFG spectra for all pH values are compared in panel (D). Spectra are offset for easier comparison. All measurements employed PPP vSFG geometry, are normalized with respect to the IR profile, and are Fresnel factor corrected.

for heterogeneously charged mineral oxide samples, suggesting that a local probe of the electrostatic potential could be more informative than streaming potential measurements, which measure the average surface property.[54]

In this work we use potassium thiocyanate, a reporter of local electrostatic potentials, to investigate the heterogeneous development of the surface charge at the α-$Al_2O_3(0001)/H_2O$ interface as the bulk pH is modulated (Figure 1).[38] We also investigate the adsorption behavior of the SCN^- at the interface at a range of bulk pH values. Quantitative analysis of the vSFG spectra indicate that at all surface charge conditions one common SCN^- species, as well as another SCN^- species unique to each surface charge of varying relative orientation, exists at the α-$Al_2O_3(0001)/H_2O$ interface. By extracting the vibrational Stark shifts from the spectral fitting, we can correlate the vSFG response of SCN^- ions experiencing the charged and neutral surface sites and determine local potentials of +308 and −154 mV assigned to positively and negatively charged aluminol groups, respectively. Density functional theory−molecular dynamics (DFT-MD) simulations of SCN^- near the α-$Al_2O_3(0001)/H_2O$ interface show that the vSFG response in the C≡N stretch region originates from a $SCN^-\cdots$H−O−Al complex, supporting the surface-site specificity of these experiments. Deconvolution of the individual amplitude and phase of thiocyanate species achieved by quantitative analysis of the vSFG spectra facilitates simultaneous measurement of the behavior (e.g., adsorption isotherms) from ions experiencing neutral and charged surface sites, allowing for in situ characterization of heterogeneously charged surfaces. The ability to measure the local electrostatic potential of heterogeneously charged solid/aqueous interfaces in situ using a nondestructive spectroscopic technique should prove useful for a wide audience.

EXPERIMENTAL SECTION

Sample Preparation. Acidic and basic H_2O solutions were made using concentrated HCl (Sigma-Aldrich, Trace SELECT grade) and NaOH (Fluka Analytical, analytical grade), respectively. These solutions were added dropwise while measuring the pH of KSCN solutions to adjust the pH. The contribution to the total ionic strength from the pH-adjusting solutions was at most 1% at the lowest KSCN concentration used. The BioXtra-grade potassium thiocyanate used was 99.0% pure (Sigma-Aldrich). Additional sample preparation details can be found in the Supporting Information.

Optical Setup/Data Normalization. The optical setup and data-normalization techniques have been described previously.[2,3] Details can be found in the Supporting Information.

Computational Details. We modeled KSCN at the α-$Al_2O_3(0001)/H_2O$ interface, initializing the system with ClayFF[55,56] and KSCN parameters from Vincze et al.[57] The α-$Al_2O_3(0001)$ slab was cleaved from the crystalline geometry with one unit cell and an O-terminated surface, which we passivated with H and replicated to obtain a surface area of (8.25 × 9.25) Å. We combined this slab with 128 H_2O molecules and one pair of K^+ and SCN^- ions in a unit cell with a z dimension of 50 Å, generating initial positions with PACKMOL.[58] We ran an NVT simulation for 1 ns and then an NPTz simulation for 1 ns to determine the z lattice value (36.81 Å). We then deformed the unit cell to this length over a 1 ns period and finally equilibrated the system in the NVT ensemble for 1 ns.

We subsequently performed Car−Parrinello molecular dynamics (CPMD) simulations using Quantum Espresso (v. 6.2.1), the SCAN[59] functional, HSCV pseudopotentials,[60] an electron mass of 200 au, and a time step of 1.0 au. We initially ran a combination of NVT and NVE simulations with a 90 Ry cutoff to equilibrate the structure followed by a production simulation for 4 ps with a cutoff of 130 Ry.

We calculated the SFG spectrum from the MD simulations and the TholeL model to compute the polarizabilities.[61] The dipole moment of the system is computed by using a variant of the QEQ method[62] with the Mulliken electronegativities and fitted idempotential parameters constrained to best reproduce the dipole moments of the TABS database.[63] To compute the response of only one surface, we apply a profile to the atomic charges and effective polarizabilities, such that only the atoms that are within 19 Å of the interface contribute to the vSFG spectrum.

The vSFG spectrum is computed as a Fourier transform of the correlation function between the polarizability and the dipole moment derivatives (eq 1),

$$\chi^{(2)}(\omega) = \mathcal{F}[\langle \dot{\alpha}(t)\dot{\mu}(0)\rangle] \quad (1)$$

where $\dot{\alpha}(t)$ is the time derivative of the polarizability and $\dot{\mu}(t)$ is the time derivative of the dipole moment. To remove any origin dependence of the dipole moment, we compute $\dot{\mu}(t)$ as

$$\dot{\mu}(t) = \sum_i [\dot{r}_i(t)q_i(t) + r_i(t)\dot{q}_i(t)] \quad (2)$$

https://dx.doi.org/10.1021/jacs.0c01366
J. Am. Chem. Soc. 2020, 142, 12096−12105

RESULTS AND DISCUSSION

To characterize thiocyanate ion adsorption at the charged and neutral α-$Al_2O_3(0001)/H_2O$ interface, we performed steady-state vSFG measurements as a function of bulk pH and KSCN concentration. Steady-state spectra show resonant features with central frequencies in the ~2100−2130 cm^{-1} range. These features grow in amplitude as the concentration is increased from 0.01 to 4 M. The features are also broad, with a FWHM of ~100 cm^{-1} at concentrations > 0.5 M. By varying the bulk pH, the surface charge of the α-$Al_2O_3(0001)$ substrate is modulated by protonating/deprotonating the surface aluminol groups.[7] We stress that at pH 6 the surface should have a net neutral surface charge.[64]

For all spectra presented in Figure 2, the central frequency of the resonant species appears to follow this trend: $\omega_{pH4} < \omega_{pH6} < \omega_{pH10}$. There is also a broad featureless contribution to the spectra in the ~1950−2250 cm^{-1} spectral region, which is more apparent at lower concentrations (0.01−0.5 M) and has a bulk pH dependence (Figure S1). Its spectral profile is similar to the H_2O bend plus libration combination mode of bulk water.[65] Because of the relatively flat nature of the spectrum, with and without electrolyte solution in the ~2100 cm^{-1} region (Figures S1 and S2), we assign the resonant features to the thiocyanate ion.

Because the C≡N stretch frequency of thiocyanate ions is sensitive to the local electrostatic potential, the ω_{SCN-} was monitored using the vSFG response as a function of surface charge.[38,45,47,66] At pH = 6, where the interface is neutral, the spectra (Figure 2) at the lowest concentration (0.1 M) display a resonant feature at ~2160 cm^{-1}. At concentrations > 0.5 M, a second feature appears at ~2110 cm^{-1} in addition to the ~2160 cm^{-1} peak, which becomes dominant in the 1−4 M KSCN spectra. At the positively charged interface (pH = 4), lower-concentration spectra (0.01−0.1 M) appear to contain two features with central frequencies at ~2075 and ~2125 cm^{-1}. At higher concentrations (>0.5 M), the spectra merge into a single feature at ~2100 cm^{-1}. For pH = 10 (negatively charged surface), a resonant feature does not become distinguishable from the nonresonant background until 0.5 M. At concentrations of 0.5−4 M, the pH = 10 spectra also appear to have a bimodal character, with two resonant features at ~2050−2065 and ~2135−2150 cm^{-1}. Concentration-dependent spectra for all bulk pH values investigated can be found in Figure S3. Steady-state vSFG spectra of KSCN at the α-$Al_2O_3(0001)/H_2O$ interface show that the thiocyanate ion's vibrational frequency is sensitive to the surface charge and suggest that more than one species exists at all bulk pH values studied.

VSFG lineshapes are sensitive to the orientation of the contributing species, and the unique shape of the vSFG response in the low-concentration regime (0.1−0.5 M) at various bulk pH values prompted further analysis of the steady-state vSFG spectra.[67] The Fano-like spectral lineshapes observed for 0.1 M KSCN pH 4 spectra and 0.5 M KSCN pH 10 spectra (Figure 3) were unexpected, as even at working electrodes this behavior has not been observed.[45−47] Because vSFG spectroscopy samples the squared modulus of all resonant responses within the IR pulse bandwidth, spectral interference can be observed in vSFG spectra, especially at charged interfaces.[32] The pH 6 KSCN vSFG spectra do not contain this behavior but possess a shoulder that is blue-shifted compared to the central peak. Spectral interference patterns are more apparent in low-concentration (0.01−0.5 M) KSCN

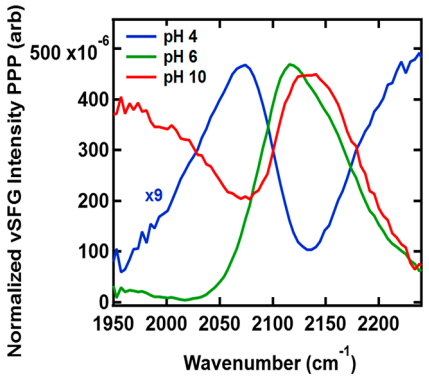

Figure 3. vSFG spectra of KSCN solutions at the α-$Al_2O_3(0001)/H_2O$ interface using PPP experimental geometry. These spectra display spectral interference patterns for 0.1 M pH 4 spectra (blue) and 0.5 M pH 10 spectra (red) with 1 M pH 6 spectra (green) for comparison.

vSFG spectra at the positively (pH 4) and negatively (pH 10) charged interface, as seen by the Fano-like up−down (pH 4) and down−up (pH 10) shape of the vSFG response. The vSFG lineshapes displayed by KSCN at the positively and negatively charged interfaces could arise from two possibilities: (a) one species interfering with the χ_{NR} contribution (Figure S4) or (b) two species with opposite net orientations at the interface.

We determine how the interfacial structure yields the observed Fano-like vSFG response by fitting the normalized vSFG response of SCN^- molecules at the interface using eq 3,

$$I_{SFG} \propto |\chi^{(2)}|^2 I_{Vis} I_{IR} = \left| \chi_{NR}^{(2)} e^{i\phi_{NR}} + \sum_{\nu} \chi_{R}^{(2)} \right|^2 I_{Vis} I_{IR}$$
$$= \left| \chi_{NR}^{(2)} e^{i\phi_{NR}} + \sum_{\nu} \frac{A_\nu}{\omega_{IR} - \omega_\nu + i\Gamma_\nu} \right|^2 I_{Vis} I_{IR} \quad (3)$$

where $\chi_{NR}^{(2)}$ and $\chi_{R}^{(2)}$ represent the nonresonant instantaneous electronic response of the system and the vibrationally resonant modes summed over the available infrared bandwidth, respectively. The ϕ term denotes the phase between the $\chi_{NR}^{(2)}$ and $\chi_{R}^{(2)}$ responses of the system. Each vibrationally resonant mode possesses a Lorentzian lineshape, where ω_{IR} is the frequency of the driving infrared pulse and A_ν, ω_ν, and Γ_ν are the amplitude, central frequency, and damping coefficient of the ν^{th} vibrational mode, respectively.

Two Lorentzian oscillators of opposite amplitude were required to properly fit the KSCN spectra at the α-$Al_2O_3(0001)/H_2O$ interface for all the pH values studied using eq 3 (Figure 4, Figures S5−S7, and Tables S1−S3). The spectral contributions from the oscillators with the larger positive amplitudes were assigned as the major contribution because their shape qualitatively best described the total vSFG response. Resonant oscillators with the negative smaller amplitudes were denoted as minor species, as these peaks mainly interfere with the dominant contribution, giving rise to the asymmetry present in the total vSFG response. The ~2100 cm^{-1} central frequency of the major peaks appears to have no concentration or surface-charge dependence (Figure 4A and C), while the central frequencies of the minor peaks vary slightly with increasing concentration and are affected by the surface charge (Figure 4B and D). The major and minor

https://dx.doi.org/10.1021/jacs.0c01366
J. Am. Chem. Soc. 2020, 142, 12096−12105

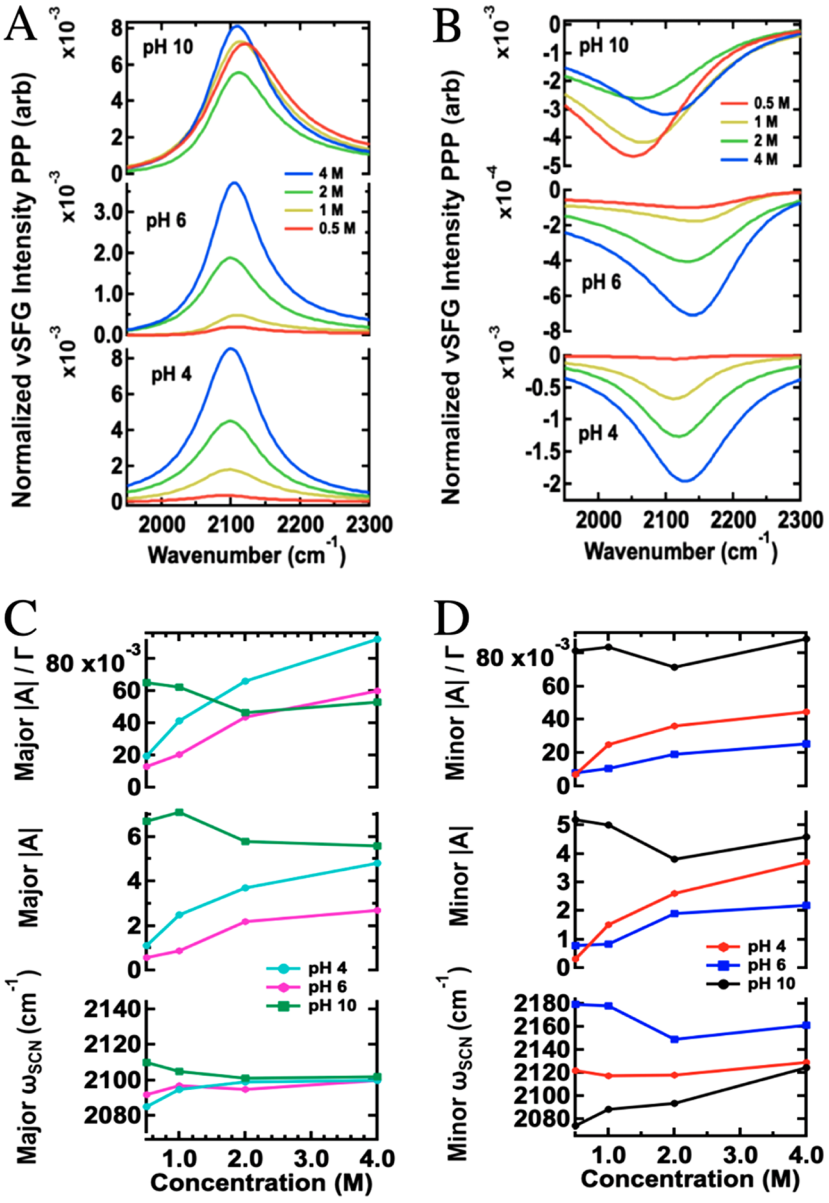

Figure 4. Lorentzian lineshapes extracted from fitting the normalized vSFG data presented in Figure 2 using eq 3. All fits required two oscillators of opposite amplitudes. The positive amplitude peaks were classified as the major contributions (A), while the negative amplitude features were denoted as minor contributions (B). The fit parameters are graphically shown versus concentration for the dominant (C) and minor (D) peaks. The tabulated fit parameter values can be found in the Supporting Information.

contributors also have opposite signs associated with their amplitudes, indicating that the net orientation at the interface is opposite to one another. The absolute values of the amplitudes divided by the damping constant, Γ_ν, are also plotted because at resonance the $\chi_R^{(2)}$ contribution reduces to this quantity. While all pH 4 and pH 6 extracted amplitudes appear to follow Langmuir adsorption (Figures S8 and S9 and Table S4), the pH 10 spectral amplitudes remain relatively constant (Figure 4C). The behavior exhibited by SCN^- at pH 10 is discussed in detail later.

The extracted vSFG central frequencies of the major and minor SCN^- species suggest that thiocyanate ions in the interfacial region experience multiple distinct local environments, which can be independently sampled simultaneously. The broad nature (~100 cm^{-1}) of the vSFG response suggests that SCN^- experiences a more heterogeneous local environment than that observed for SAMs at working electrodes.[45−47,66] The bandwidth of the observed vSFG features is similar to that reported for SCN^- at the electrode interfaces (~150 cm^{-1}).[38,68] The extracted width (Γ_n) of the minor species led us to consider its identity as the bend plus libration combination mode of H_2O, but spectral shifts as large as those observed in our vSFG measurements versus electrolyte concentration have not been reported in previous bulk IR studies.[65] In addition, recent work suggests that vSFG spectral density in the 1700−3000 cm^{-1} region arises mainly from nonresonant contributions, which could not be reproduced computationally by including solvated H^+, OH^-, or the bend plus libration combination mode.[69] In addition to these concerns, the probability of probing a combination band is much lower than the C≡N stretch and a strong IR Raman-active mode. Hence, we conclude that the multiple resonant contributions to the vSFG response originate from the

https://dx.doi.org/10.1021/jacs.0c01366
J. Am. Chem. Soc. 2020, 142, 12096−12105

response of thiocyanate species experiencing distinct local environments.

The concentration-dependent vSFG response can track the adsorption behavior of thiocyanate species in the interfacial region.[70] However, the broad nonresonant background in the 0.01−0.5 M KSCN spectra made direct comparison difficult, leading us to fit this vSFG data using eq 3. The extracted amplitudes (Figure 4C and D) describe the adsorption affinity of thiocyanate species at varied KSCN concentrations and surface charges. Both the major and minor species present at bulk pH = 4 and 6 appear to exhibit Langmuir adsorption (Figure S8). While all of the assumptions of the Langmuir adsorption model are not fulfilled by our interface, fitting the data using this model as an approximation can provide information regarding the relative surface affinity of SCN^- at various bulk pH values. The pH 6 major and minor isotherms yielded ΔG_{Ads} values of −6.5 and −8.0 kJ/mol, while adsorption of the pH 4 major and minor gave values of −7.9 and −5.7 kJ/mol, respectively (Table S4). At pH 10, however, the extracted amplitudes associated with the major and minor species remain relatively constant. The plotted A_ν/Γ_ν versus concentration suggest that thiocyanate species adsorb more rapidly under pH = 4 conditions compared to pH = 6.

While the adsorption of thiocyanate at the positively charged α-$Al_2O_3(0001)/H_2O$ interface is consistent with Coulombic attraction, the behavior at the neutral and negatively charged interfaces requires additional explanation. The Langmuir isotherm exhibited by pH 6 species suggests adsorption at surface aluminol sites is energetically favorable (Figure S5). At pH 10, however, the extracted amplitudes suggest that SCN^- species have saturated the surface at nearly all concentrations, and the amplitude of the detected species remains similar (Figure 4C and D). We hypothesize that the approach of SCN^- ions toward the negatively charged surface is facilitated through $K^+\cdots SCN^-$ ion pair interactions because the approach of an anion toward the negatively charged surface must be Coulombically hindered.[2] This could be accomplished by primary adsorption of cations, with accompanying attraction of the counterion SCN^-.[23] The extracted amplitudes from fitting of pH 10 KSCN vSFG spectra suggest that the effect of cation adsorption on SCN^- attraction to the α-$Al_2O_3(0001)/H_2O$ interface is saturated at all concentrations tested here. This is supported by the fact that K^+ has a high adsorption affinity for the negatively charged α-$Al_2O_3(0001)$ surface, previously demonstrated by a 2 orders of magnitude attenuation of the vSFG response in the O−H stretching region by 0.1 M KCl solutions.[23]

While the manner in which Al_2O_3 surface sites contribute to the vSFG spectra in the OH stretching region remains controversial, it is widely accepted that the aqueous surface is terminated with AlOH surface groups that adopt two main configurations: ∼60% in the plane of the substrate and ∼40% pointing out of the plane.[25,71,72] We recover approximately the same ratio of in- and out-of-plane aluminols by integrating the generated angular distribution function from the simulated α-$Al_2O_3(0001)/H_2O$ interface (Figure S10). To unravel the origin of the local surface charge heterogeneity associated with these adsorption sites, the percentage of aluminol groups that are charged at bulk pH = 4 and pH = 10 must be considered. The average surface charge of α-$Al_2O_3(0001)$ particles versus bulk pH values has been characterized via potentiometric titrations.[64] Using this data,[64] and the fact that the α-$Al_2O_3(0001)$ surface is terminated with ∼15 aluminol groups/nm^2,[5,6] as well as that charges are localized on AlO^- or $AlOH_2^+$ sites, one can infer the number density per unit area of charged surface sites at pH 4 and pH 10. Ntalikwa reported a surface charge densities of 2×10^{-19} and -1×10^{-19} C/nm^2 for bulk pH 4 and pH 10 solutions, respectively.[64] If every charged site generates 1 unit of elementary charge, this suggests that, at pH = 4, ∼1.25 aluminol groups/nm^2 are protonated and, at pH = 10, ∼0.63 aluminol groups/nm^2 are deprotonated. This can be compared to the surface coverage parameter $\theta([\chi_{bulk}])$ extracted from a Langmuir fit of the extracted SFG amplitudes for each thiocyanate species (Figure S11). The tabulated results suggest that, for our experimental conditions, the maximum surface coverage densities for pH 4 and pH 6 major and minor species range from 0.83 to 1.28 SCN^- reporter ions/nm^2 (Table S5). The relatively small number of charged sites at the surface, coupled with the inability to redistribute surface charges homogeneously across the insulating surface, implies that locally Stark active ions would experience multiple distinct binding sites.

To quantify the local electrostatic potential associated with the charged aluminol groups, we use the reported Stark tuning rate for SCN^- ions via SFG measurements of 65 cm^{-1}/V corresponding to an externally applied bias across a platinum electrode.[38,73,74] While the interaction of SCN^- with a platinum working electrode is certainly different in nature than that with insulating oxide surfaces, the response of reporter ions to a known applied potential is required for the deductions made here. As stated earlier, the majority of aluminol groups remain neutral at all pH values used in this work. For this reason, we attribute the largest, concentration-independent amplitude at ∼2100 cm^{-1} for all bulk pH values to SCN^- adjacent to neutral AlOH sites, which we assign to a local potential of ∼0 V. As in streaming potential measurements, this choice of 0 V potential serves as a reference because, at all bulk pH values explored here, neutral (0 V) sites are present, while the average surface potential varies with bulk pH.[7] The addition of KSCN can, in principle, affect the interfacial electrostatic potential. When KSCN vSFG spectra in the OH stretching region (Figure S12) are compared to monovalent halide ions (Figure S13), the concentration-dependent spectral profiles appear to be similar, suggesting that the behavior of KSCN is comparable to that of halide species.[75] Because halide ions do not appear to affect the surface charge of the α-$Al_2O_3(0001)/H_2O$ interface,[76] we propose that the SCN^- ion can be used to measure the local potential without impacting the net surface charge. The IR spectra and vSFG spectra of KSCN at pH 6 in the bulk and at the α-$Al_2O_3(0001)/H_2O$ interface for the C≡N spectral region can be found in the Supporting Information. The vSFG response of SCN^- at the pH 6 interface is blue-shifted by 33 cm^{-1} compared to the IR signature in bulk H_2O (Figure S14), which we hypothesize originates from differences between the bulk and the interfacial dielectric constants. If we consider the average values of 2122, 2167, and 2095 cm^{-1} for pH 4, 6, and 10 KSCN minor species, respectively, and apply the 65 cm^{-1}/V Stark tuning rate, these values correspond to local potentials of +0.308, +0.923, and −0.154 V, respectively.

Here we discuss the origin the potential sensed at pH 4 and pH 10 conditions. Potentiometric titrations of α-$Al_2O_3(0001)$ powders suggest that ∼1.25 aluminol groups protonated per nm^2 at pH 4 and ∼0.63 aluminol groups deprotonated per nm^2 at pH 10.[64] If the ∼2.5 Å long SCN^- ions can sense multiple charged groups simultaneously, then this suggests that the field

https://dx.doi.org/10.1021/jacs.0c01366
J. Am. Chem. Soc. 2020, 142, 12096−12105

strengths associated with both protonated and deprotonated aluminol sites are on the order of ~150 mV per group, because twice as many aluminols are charged at pH 4 compared to pH 10 conditions. DFT-based theoretical studies, however, have suggested that Cl^- is only able to disrupt local water molecules within two hydration shells, which suggests that SCN^- ions should only be affected by one charged aluminol group at any time, at the density estimated.[77] In this scenario, the potentials measured from the protonated and deprotonated aluminol groups would be +308 and −154 mV, respectively. It should be noted that the presence of K^+ counterions near the negative sites could influence the potential sensed by thiocyanate ions at pH 10, but currently this cannot be revealed by our experimental or theoretical methods.

The distance of the SCN^- reporter ions from the charged sites would affect the potential sensed. While vSFG cannot spatially resolve the position of SCN^-, previous vSFG experiments at the SiO_2/H_2O and α-$Al_2O_3(0001)/H_2O$ interfaces suggest that vSFG is sensitive to only the first few layers of interfacial solvent so that the SCN^- is likely at most 1 nm from the sites whose potential it reports and probably much less.[2,18,78] We have also included a calculation of the distance-dependent Coulomb potential using different values for the dielectric constant of the interface (Figure S15) to show that SCN^- are likely <5 Å away from charged sites at pH 4 and pH 10. Our DFT-MD simulations and vSFG spectra are consistent with the largest component of the vSFG response at all pH values originating from SCN^- hydrogen-bonding with neutral AlOH sites, further providing evidence of the surface specificity of the results provided here. We hypothesize that thiocyanate species experience the potential of one charged aluminol group at a time, as generating like charges in close proximity to one another should be unfavorable. These results suggest that SCN^- ions sense the entire local electric field near the positively charged aluminol groups and a partially screened charge, likely by K^+, near the deprotonated aluminol groups.

To understand the origin of the ~60 cm^{-1} shift associated with the pH 6 minor species, we look to the literature and our DFT-MD results for guidance. Recent work has shown similar differences in the stretching-mode frequencies of Stark active molecules in the Stern and diffuse layers.[47] However, we do not believe this is an adequate explanation for our results, as at high salt concentrations the diffuse layer should be quite short, and the amplitude of this peak would be expected to decline with increasing electrolyte concentration. As stated earlier, one could interpret the fitted pH 6 vSFG spectra to suggest that a subpopulation of SCN^- ions sense a +0.923 V potential near surface sites; however, this is unlikely due to the small number of charged aluminol groups present at neutral pH as indicated by the PZC. Instead, we hypothesize that at pH 6 the minor population originates from K^+SCN^- ion pairs. The close proximity between ion-pair partners could be the origin of the nearly +1 V sensed and the large blue-shift of the CN frequency of thiocyanate ions participating in contact ion pairs. Careful inspection of Figure S3A shows that the ~2160 cm^{-1} species in pH 6 spectra is present before the 2100 cm^{-1} species becomes separable from the nonresonant background. This suggests that at low concentrations ion pairs adsorb more favorably at the nominally neutral surface, consistent with estimations that the interfacial dielectric constant is lower than the corresponding bulk value (~80), a factor that enhances ion-pair binding.[79,80] The large spectral blue-shift associated with contact ion pairs at pH 6 is also supported by our DFT-MD calculations, as the vibrational frequency derived from the VDOS for SCN^- is nearly 200 cm^{-1} red-shifted compared to HSCN. While this shift is large, it supports the notion that the contact ion pairs have vibrational frequencies that are blue-shifted compared to groups interacting with aluminol groups, consistent with bulk experiments.[43] Thus, we believe that the minor population at pH 6 originates from KSCN ion pairs. It remains unclear why ion pairs were not detected at bulk pH 4 and pH 10 conditions.

The localized nature of the protonated and deprotonated aluminol sites leads to large local potentials experienced by adsorbed SCN^- molecules. The same charge homogeneously spread across a conductive substrate would lead to a much smaller potential and associated vibrational Stark shift. Using the extracted amplitudes from the fitted vSFG response for major and minor lineshapes, and cross referencing with the orientation sampled by pH 6 DFT-MD simulations, we can propose relative orientations of all four species sampled in our vSFG measurements (Figure 5). Our DFT-MD simulations

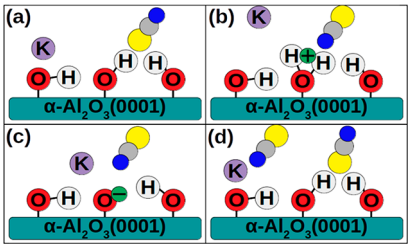

Figure 5. Proposed schematic of all four thiocyanate species sampled at the α-$Al_2O_3(0001)$ interface. The major contribution to the vSFG spectra, which exists at all bulk pH values, is shown in (A), while (B), (C), and (D) depict the minor contributions from species only sampled at pH 4, 10, and 6, respectively.

suggest that thiocyanate species interacting with aluminol groups at pH 6 adopt an orientation with the S atom pointing toward the alumina substrate. This orientation is correlated with the positive amplitude fit results, and negative amplitudes associated with the minor species must then represent a net N atom down orientation. This picture is consistent with the Coulombic attraction of the more electronegative N atom with the positively charged sites and is compatible with an aluminol···K^+···$^-$NCS complex at pH 10. We hypothesize that the SCN^- ions contributing to the minor lineshapes at pH = 4 and 10 are in close proximity to charged sites and are drawn to these sites first. Evaluation of the Langmuir adsorption isotherms for pH 4 and pH 6 major and minor species suggest that all four species spontaneously adsorb on the surface, yet all share similar ΔG_{Ads} values (−5.7 to −8.0 kJ/mol). This analysis was not possible at pH 10 because of the flat nature of the adsorption isotherm for both pH 10 major and minor species, which could be obscured by SCN^-···K^+ interactions near the surface. Increasing the concentration of SCN^- should not change the inherent nature of these charged surface sites, consistent with the stability of the central frequency of SCN^- ions contributing to the minor lineshapes at pH 4 and pH 10. The gradual blue-shift in the pH 10 minor central frequency (Figure 4D) is attributed to accumulation of the counterion (K^+) at the surface, which can efficiently screen interfacial charges, leading to a smaller potential emanating from the negatively charged aluminol groups.[23]

https://dx.doi.org/10.1021/jacs.0c01366
J. Am. Chem. Soc. 2020, 142, 12096−12105

CONCLUSION

vSFG spectra of potassium thiocyanate, a reporter of the local electrostatic potential, were recorded at the α-Al_2O_3(0001)/H_2O interface as a function of bulk pH and KSCN concentration. Steady-state vSFG spectra show accumulation of SCN^- ions at concentrations as low as 0.1 M. The vSFG spectral peak position and shape are sensitive to the surface charge. Deconvolution of normalized vSFG data via spectral fitting shows that, at all surface-charge values, one species with its S atom oriented toward the substrate is conserved, while a total of three different species with S pointed toward the bulk were identified, each unique to bulk pH 4, 6, and pH 10 conditions. The steady-state vSFG spectra allow adsorption at charged and neutral sites to be tracked independently and show that adsorption of thiocyanate species is spontaneous with a Gibbs free energy of approximately −7 kJ/mol. DFT-MD simulations of SCN^- near the α-Al_2O_3(0001)/H_2O interface suggest that the major peak's frequency of ∼2100 cm^{-1} can be attributed to the SCN^- molecules hydrogen-bonding with neutral aluminol groups. Two minor species exist at pH 4 and pH 10 and are assigned to the SCN^- molecular ions experiencing local electrostatic potentials of +0.308 and −0.154 V associated with protonated and deprotonated aluminol groups, respectively. The secondary species at pH 6, which is ∼60 cm^{-1} blue-shifted from the SCN^- ions experiencing neutral sites, is attributed to K^+SCN^- contact ion pairs. By directly probing the surface aluminol groups, whose nature has been highly controversial due to the difficulty of spectroscopically accessing them directly, we are able to assign local potentials to the various charged and neutral sites on the α-Al_2O_3(0001) surface. To our knowledge this is the first spectroscopic measurement of local potentials associated with heterogeneously charged surfaces, and the ability to measure the heterogeneous charge evolution of working surfaces could prove highly beneficial for future technologies using mineral oxide nanoparticles as catalytic supports, monitoring the charge evolution of nanoelectrode devices in real time, and many other industrial and academic applications.

ASSOCIATED CONTENT

Supporting Information

The Supporting Information is available free of charge at https://pubs.acs.org/doi/10.1021/jacs.0c01366.

Information regarding experimental details, computational parameters, and data processing; additional experimental and simulated SFG spectra of aqueous solutions with and without electrolyte at the α-Al_2O_3(0001) interface; simulation of a pair of Lorentzian lineshapes in-phase and out-of-phase; Langmuir adsorption isotherms of KSCN vSFG spectra at the α-Al_2O_3(0001)/H_2O interface; and distance-dependent Coulomb potentials for different dielectric constant values (PDF)

AUTHOR INFORMATION

Corresponding Author

Eric Borguet − *Department of Chemistry and Center for Complex Materials from First-Principles, Temple University, Philadelphia, Pennsylvania 19122, United States;* orcid.org/0000-0003-0593-952X; Email: eborguet@temple.edu

Authors

Stefan M. Piontek − *Department of Chemistry, Temple University, Philadelphia, Pennsylvania 19122, United States;* orcid.org/0000-0001-9564-6258

Mark DelloStritto − *Institute for Computational Molecular Science, Temple University, Philadelphia, Pennsylvania 19122, United States;* orcid.org/0000-0002-0678-5860

Bijoya Mandal − *Department of Chemistry, Temple University, Philadelphia, Pennsylvania 19122, United States*

Tim Marshall − *Department of Chemistry, Temple University, Philadelphia, Pennsylvania 19122, United States*

Michael L. Klein − *Institute for Computational Molecular Science and Center for Complex Materials from First-Principles, Temple University, Philadelphia, Pennsylvania 19122, United States*

Complete contact information is available at: https://pubs.acs.org/10.1021/jacs.0c01366

Notes

The authors declare no competing financial interest.

ACKNOWLEDGMENTS

The authors acknowledge and thank the National Science Foundation (NSF Grant MRI 1828421) and the American Chemical Society Petroleum Research Fund (PRF no. 58559-ND5) for supporting this work. M.D. gives thanks for support from the Computational Chemical Center: Chemistry in Solution and at Interfaces funded by the DOE under Award DE-SC0019394. E.B. and M.L.K. acknowledge support from the Center for Complex Materials from First-principles, an Energy Frontier Research Center funded under the Department of Energy Grant no. DE-SC0012575. The authors are thankful for Mr. Nima Khaki's work designing the TOC image. The authors also thank Professor M. Zdilla (Temple University, Chemistry Department) for alumina prism face orientation identification via X-ray diffraction and Dr. Kyle Gilroy (Professor S. Neretina Group, Temple University, College of Engineering) for gold-coating alumina prisms that were used for SFG data normalization.

REFERENCES

(1) Smits, M.; Ghosh, A.; Bredenbeck, J.; Yamamoto, S.; Muller, M.; Bonn, M. Ultrafast Energy Flow in Model Biological Membranes. *New J. Phys.* **2007**, *9*, 390.

(2) Tuladhar, A.; Piontek, S. M.; Frazer, L.; Borguet, E. Effect of Halide Anions on the Structure and Dynamics of Water Next to an Alumina (0001) Surface. *J. Phys. Chem. C* **2018**, *122* (24), 12819−12830.

(3) Tuladhar, A.; Piontek, S. M.; Borguet, E. Insights on Interfacial Structure, Dynamics, and Proton Transfer from Ultrafast Vibrational Sum Frequency Generation Spectroscopy of the Alumina(0001)/Water Interface. *J. Phys. Chem. C* **2017**, *121* (9), 5168−5177.

(4) Tuladhar, A.; Dewan, S.; Kubicki, J. D.; Borguet, E. Spectroscopy and Ultrafast Vibrational Dynamics of Strongly Hydrogen Bonded OH Species at the α-Al_2O_3(1120)/H_2O Interface. *J. Phys. Chem. C* **2016**, *120* (29), 16153−16161.

(5) Eng, P. J.; Trainor, T. P.; Brown, G. E., Jr.; Waychunas, G. A.; Newville, M.; Sutton, S. R.; Rivers, M. L. Structure of the Hydrated α-Al_2O_3 (0001). *Science* **2000**, *288* (5468), 1029−1033.

(6) Hass, K. C.; Schneider, W. F.; Curioni, A.; Andreoni, W. First-Principles Molecular Dynamics Simulations of H_2O on α-Al_2O_3 (0001). *J. Phys. Chem. B* **2000**, *104* (23), 5527−5540.

(7) Lutzenkirchen, J.; Franks, G. V.; Plaschke, M.; Zimmermann, R.; Heberling, F.; Abdelmonem, A.; Darbha, G. K.; Schild, D.; Filby, A.;

Eng, P.; Catalano, J. G.; Rosenqvist, J.; Preocanin, T.; Aytug, T.; Zhang, D.; Gan, Y.; Braunschweig, B. The Surface Chemistry of Sapphire-C: A Literature Review and a Study on Various Factors Influencing its IEP. *Adv. Colloid Interface Sci.* **2018**, *251*, 1−25.
(8) Yeganeh, M. S.; Dougal, S. M.; Pink, H. S. Vibrational Spectroscopy of Water at Liquid/Solid Interfaces: Crossing the Isoelectric Point of a Solid Surface. *Phys. Rev. Lett.* **1999**, *83* (6), 1179−1182.
(9) Zhang, L.; Tian, C.; Waychunas, G. A.; Shen, Y. R. Structures and Charging of α-Alumina (0001)/Water Interfaces Studied by Sum-Frequency Vibrational Spectroscopy. *J. Am. Chem. Soc.* **2008**, *130* (24), 7686−7694.
(10) Sprik, M.; Klein, M. L. A Polarizable Model For Water Using Distributed Charge Sites. *J. Chem. Phys.* **1988**, *89* (12), 7556−7560.
(11) McCaffrey, D. L.; Nguyen, S. C.; Cox, S. J.; Weller, H.; Alivisatos, A. P.; Geissler, P. L.; Saykally, R. J. Mechanism of Ion Adsorption to Aqueous Interfaces: Graphene/Water vs. Air/Water. *Proc. Natl. Acad. Sci. U. S. A.* **2017**, *114* (51), 13369−13373.
(12) Arrouvel, C.; Digne, M.; Breysse, M.; Toulhoat, H.; Raybaud, P. Effects of Morphology on Surface Hydroxyl Concentration: A DFT Comparison of Anatase-TiO_2 and γ-Alumina Catalytic Supports. *J. Catal.* **2004**, *222* (1), 152−166.
(13) Gorin, C. F.; Beh, E. S.; Bui, Q. M.; Dick, G. R.; Kanan, M. W. Interfacial Electric Field Effects on a Carbene Reaction Catalyzed by Rh Porphyrins. *J. Am. Chem. Soc.* **2013**, *135* (30), 11257−11265.
(14) Schmickler, W.; Santos, E. *Interfacial Electrochemistry*, second ed.; Springer: New York City, 2010.
(15) Sivula, K. Metal Oxide Photoelectrodes for Solar Fuel Production, Surface Traps, and Catalysis. *J. Phys. Chem. Lett.* **2013**, *4* (10), 1624−1633.
(16) Hisatomi, T.; Kubota, J.; Domen, K. Recent Advances in Semiconductors for Photocatalytic and Photoelectrochemical Water Splitting. *Chem. Soc. Rev.* **2014**, *43* (22), 7520−7535.
(17) Meille, V. Review on Methods to Deposit Catalysts on Structured Surfaces. *Appl. Catal., A* **2006**, *315*, 1−17.
(18) Eftekhari-Bafrooei, A.; Borguet, E. Effect of Surface Charge on the Vibrational Dynamics of Interfacial Water. *J. Am. Chem. Soc.* **2009**, *131* (34), 12034−12035.
(19) Du, Q.; Freysz, E.; Shen, Y. R. Vibrational Spectra of Water Molecules at Quartz/Water Interfaces. *Phys. Rev. Lett.* **1994**, *72* (2), 238−241.
(20) Tian, C. S.; Shen, Y. R. Structure and Charging of Hydrophobic Material/Water Interfaces Studied by Phase-Sensitive Sum-Frequency Vibrational Spectroscopy. *Proc. Natl. Acad. Sci. U. S. A.* **2009**, *106* (36), 15148−15153.
(21) Flores, S. C.; Kherb, J.; Konelick, N.; Chen, X.; Cremer, P. S. The Effects of Hofmeister Cations at Negatively Charged Hydrophilic Surfaces. *J. Phys. Chem. C* **2012**, *116* (9), 5730−5734.
(22) Ong, S. W.; Zhao, X. L.; Eisenthal, K. B. Polarization of Water-Molecules at a Charged Interface - 2nd Harmonic Studies of the Silica Water Interface. *Chem. Phys. Lett.* **1992**, *191* (3−4), 327−335.
(23) Piontek, S. M.; Tuladhar, A.; Marshall, T.; Borguet, E. Monovalent and Divalent Cations at the α-Al_2O_3(0001)/Water Interface: How Cation Identity Affects Interfacial Ordering and Vibrational Dynamics. *J. Phys. Chem. C* **2019**, *123* (30), 18315−18324.
(24) Darlington, A. M.; Jarisz, T. A.; DeWalt-Kerian, E. L.; Roy, S.; Kim, S.; Azam, M. S.; Hore, D. K.; Gibbs, J. M. Separating the pH-Dependent Behavior of Water in the Stern and Diffuse Layers with Varying Salt Concentration. *J. Phys. Chem. C* **2017**, *121* (37), 20229−20241.
(25) DelloStritto, M.; Sofo, J. Bond Polarizability Model for Sum Frequency Generation at the Al_2O_3(0001)-H_2O Interface. *J. Phys. Chem. A* **2017**, *121* (16), 3045−3055.
(26) Chattopadhyay, A.; Boxer, S. G. Vibrational Stark-Effect Spectroscopy. *J. Am. Chem. Soc.* **1995**, *117* (4), 1449−1450.
(27) Lambert, D. K. Vibrational Stark Effect of Adsorbates at Electrochemical Interfaces. *Electrochim. Acta* **1996**, *41* (5), 623−630.
(28) Lambert, D. K. Vibrational Stark Effect of CO On Ni(100) and CO In the Aqeuous Double-Layer - Experiment, Theory, and Models. *J. Chem. Phys.* **1988**, *89* (6), 3847−3860.
(29) Wasileski, S. A.; Koper, M. T. M.; Weaver, M. J. Field-Dependent Electrode-Chemisorbate Bonding: Sensitivity of Vibrational Stark Effect and Binding Energetics to Nature of Surface Coordination. *J. Am. Chem. Soc.* **2002**, *124* (11), 2796−2805.
(30) Weaver, M. J.; Wasileski, S. A. Influence of Double-Layer Solvation on Local Versus Macroscopic Surface Potentials on Ordered Platinum-Group Metals as Sensed by the Vibrational Stark Effect. *Langmuir* **2001**, *17* (10), 3039−3043.
(31) Fitts, J. P.; Shang, X. M.; Flynn, G. W.; Heinz, T. F.; Eisenthal, K. B. Electrostatic Surface Charge at Aqueous/α-Al_2O_3 Single-Crystal Interfaces as Probed by Optical Second-Harmonic Generation. *J. Phys. Chem. B* **2005**, *109* (16), 7981−7986.
(32) Ohno, P. E.; Wang, H. F.; Geiger, F. M. Second-Order Spectral Lineshapes from Charged Interfaces. *Nat. Commun.* **2017**, *8*, 1032.
(33) Bagchi, S.; Fried, S. D.; Boxer, S. G. A Solvatochromic Model Calibrates Nitriles' Vibrational Frequencies to Electrostatic Fields. *J. Am. Chem. Soc.* **2012**, *134* (25), 10373−10376.
(34) Suydam, I. T.; Snow, C. D.; Pande, V. S.; Boxer, S. G. Electric Fields at the Active Site of an Enzyme: Direct Comparison of Experiment with Theory. *Science* **2006**, *313* (5784), 200−204.
(35) Fried, S. D.; Boxer, S. G. Measuring Electric Fields and Noncovalent Interactions Using the Vibrational Stark Effect. *Acc. Chem. Res.* **2015**, *48* (4), 998−1006.
(36) Fried, S. D.; Boxer, S. G. Electric Fields and Enzyme Catalysis. In *Annual Review of Biochemistry*; Kornberg, R. D., Ed.; Annual Reviews: Palo Alto, CA, 2017; Vol. *86*, pp 387−415.
(37) Baldelli, S. Probing Electric Fields at the Ionic Liquid-Electrode Interface Using Sum Frequency Generation Spectroscopy and Electrochemistry. *J. Phys. Chem. B* **2005**, *109* (27), 13049−13051.
(38) Tadjeddine, A.; Guyotsionnest, P. Spectroscopic Investigation Of Adsorbed Cyanide And Thiocyanate On Platinum Using Sum Frequency Generation. *Electrochim. Acta* **1991**, *36* (11−12), 1849−1854.
(39) Schkolnik, G.; Salewski, J.; Millo, D.; Zebger, I.; Franzen, S.; Hildebrandt, P. Vibrational Stark Effect of the Electric-Field Reporter 4-Mercaptobenzonitrile as a Tool for Investigating Electrostatics at Electrode/SAM/Solution Interfaces. *Int. J. Mol. Sci.* **2012**, *13* (6), 7466−7482.
(40) Oklejas, V.; Sjostrom, C.; Harris, J. M. Surface-Enhanced Raman Scattering Based Vibrational Stark Effect as a Spatial Probe of Interfacial Electric Fields in the Diffuse Double Layer. *J. Phys. Chem. B* **2003**, *107* (31), 7788−7794.
(41) Oklejas, V.; Sjostrom, C.; Harris, J. M. SERS Detection of the Vibrational Stark Effect from Nitrile-Terminated SAMs to Probe Electric Fields in the Diffuse Double-Layer. *J. Am. Chem. Soc.* **2002**, *124* (11), 2408−2409.
(42) Kellner, R.; Zippel, E.; Pungor, E.; Toth, K.; Lindner, E. FTIR-ATR Spectroscopic Analysis Of Bis-Crown Ether Based PVC-Membranes 0.2. The Diffusion Behavior Of K^+-Complexes In The System Of PVC Dioctylsebacate Crown-Ether Bme-44 - Ex-Situ-Studies On Dried Membranes. Fresenius. *Fresenius' Z. Anal. Chem.* **1987**, *328* (6), 464−468.
(43) Guha, C.; Chakraborty, J. M.; Karanjai, S.; Das, B. The Structure and Thermodynamics of Ion Association and Solvation of Some Thiocyanates and Nitrates in 2-methoxyethanol Studied by Conductometry and FTIR Spectroscopy. *J. Phys. Chem. B* **2003**, *107* (46), 12814−12819.
(44) Hage, W.; Hallbrucker, A.; Mayer, E. Increasing Ion-Pairing And Aggregation In Supercooled And Glassy Dilute Aqueous-Electrolyte Solution As Seen By FTIR Spectroscopy Of Alkali-Metal Thiocyanates. *J. Phys. Chem.* **1992**, *96* (15), 6488−6493.
(45) Patrow, J. G.; Sorenson, S. A.; Dawlaty, J. M. Direct Spectroscopic Measurement of Interfacial Electric Fields near an Electrode under Polarizing or Current-Carrying Conditions. *J. Phys. Chem. C* **2017**, *121* (21), 11585−11592.

https://dx.doi.org/10.1021/jacs.0c01366
J. Am. Chem. Soc. 2020, 142, 12096−12105

(46) Patrow, J. G.; Wang, Y.; Dawlaty, J. M. Interfacial Lewis Acid-Base Adduct Formation Probed by Vibrational Spectroscopy. *J. Phys. Chem. Lett.* **2018**, *9* (13), 3631−3638.
(47) Ge, A. M.; Videla, P. E.; Lee, G. L.; Rudshteyn, B.; Song, J.; Kubiak, C. P.; Batista, V. S.; Lian, T. Q. Interfacial Structure and Electric Field Probed by in Situ Electrochemical Vibrational Stark Effect Spectroscopy and Computational Modeling. *J. Phys. Chem. C* **2017**, *121* (34), 18674−18682.
(48) Clark, M. L.; Ge, A. M.; Videla, P. E.; Rudshteyn, B.; Miller, C. J.; Song, J.; Batista, V. S.; Lian, T. Q.; Kubiak, C. P. CO_2 Reduction Catalysts on Gold Electrode Surfaces Influenced by Large Electric Fields. *J. Am. Chem. Soc.* **2018**, *140* (50), 17643−17655.
(49) Butt, H. J. Measuring Local Surface-Charge Densities In Electrolyte-Solutions With A Scanning Force Microscope. *Biophys. J.* **1992**, *63* (2), 578−582.
(50) Covert, P. A.; Hore, D. K. Geochemical Insight from Nonlinear Optical Studies of Mineral−Water Interfaces. In *Annual Review of Physical Chemistry*; Johnson, M. A., Martinez, T. J., Eds.; Annual Reviews: Palo Alto, CA, 2016; Vol. *67*, pp 233−257.
(51) Franks, G. V.; Meagher, L. The Isoelectric Points of Sapphire Crystals and Alpha-Alumina Powder. *Colloids Surf., A* **2003**, *214* (1−3), 99−110.
(52) Zhang, D.; Wang, Y.; Gan, Y. Characterization of Critically Cleaned Sapphire Single-Crystal Substrates by Atomic Force Microscopy, XPS and Contact Angle Measurements. *Appl. Surf. Sci.* **2013**, *274*, 405−417.
(53) Contescu, C.; Jagiello, J.; Schwarz, J. A. Heterogeneity of Proton Binding-Sites at the Oxide Solution Interface. *Langmuir* **1993**, *9* (7), 1754−1765.
(54) Stack, A. G.; Higgins, S. R.; Eggleston, C. M. Point of Zero charge of a Corundum-Water Interface Probed with Optical Second Harmonic Generation (SHG) and Atomic Force Microscopy (AFM): New Approaches to Oxide Surface Charge. *Geochim. Cosmochim. Acta* **2001**, *65* (18), 3055−3063.
(55) Cygan, R. T.; Liang, J. J.; Kalinichev, A. G. Molecular Models of Hydroxide, Oxyhydroxide, and Clay Phases and the Development of a General Force Field. *J. Phys. Chem. B* **2004**, *108* (4), 1255−1266.
(56) Wang, R.; DelloStritto, M.; Remsing, R. C.; Carnevale, V.; Klein, M. L.; Borguet, E. Sodium Halide Adsorption and Water Structure at the α-Alumina (0001)/Water Interface. *J. Phys. Chem. C* **2019**, *123* (25), 15618−15628.
(57) Vincze, A.; Jedlovszky, P.; Horvai, G. The L/L Interface and Adsorption of SCN^- Anions as Studied by Different Molecular Simulation Techniques. *Anal. Sci.* **2001**, *17*, i317−i320.
(58) Martinez, L.; Andrade, R.; Birgin, E. G.; Martinez, J. M. PACKMOL: A Package for Building Initial Configurations for Molecular Dynamics Simulations. *J. Comput. Chem.* **2009**, *30* (13), 2157−2164.
(59) Sun, J.; Ruzsinszky, A.; Perdew, J. P. Strongly Constrained and Appropriately Normed Semilocal Density Functional. *Phys. Rev. Lett.* **2015**, *115* (3), 036402.
(60) Hamann, D. R.; Schluter, M.; Chiang, C. Norm-Conserving Pseudopotentials. *Phys. Rev. Lett.* **1979**, *43* (20), 1494−1497.
(61) DelloStritto, M.; Klein, M. L.; Borguet, E. Bond-Dependent Thole Model for Polarizability and Spectroscopy. *J. Phys. Chem. A* **2019**, *123* (25), 5378−5387.
(62) Rappe, A. K.; Goddard, W. A. Charge Equilibration for Molecular-Dynamics Simulations. *J. Phys. Chem.* **1991**, *95* (8), 3358−3363.
(63) Blair, S. A.; Thakkar, A. J. TABS: A Database of Molecular Structures. *Comput. Theor. Chem.* **2014**, *1043*, 13−16.
(64) Ntalikwa, J. W. Determination of Surface Charge Density of α-Alumina by Acid-Base Titration. *Bull. Chem. Soc. Ethiop.* **2007**, *21* (1), 117−128.
(65) Verma, P. K.; Kundu, A.; Puretz, M. S.; Dhoonmoon, C.; Chegwidden, O. S.; Londergan, C. H.; Cho, M. The Bend plus Libration Combination Band is an Intrinsic, Collective, and Strongly Solute-Dependent Reporter on the Hydrogen Bonding Network of Liquid Water. *J. Phys. Chem. B* **2018**, *122* (9), 2587−2599.
(66) Sorenson, S. A.; Patrow, J. G.; Dawlaty, J. M. Solvation Reaction Field at the Interface Measured by Vibrational Sum Frequency Generation Spectroscopy. *J. Am. Chem. Soc.* **2017**, *139* (6), 2369−2378.
(67) Wang, H. F.; Velarde, L.; Gan, W.; Fu, L. Quantitative Sum-Frequency Generation Vibrational Spectroscopy of Molecular Surfaces and Interfaces: Lineshape, Polarization, and Orientation. In *Annual Review of Physical Chemistry*; Johnson, M. A., Martinez, T. J., Eds.; Annual Reviews: Palo Alto, CA, 2015; Vol. *66*, pp 89−216.
(68) Wang, J. J.; Xu, M.; Huangfu, Z. C.; Wang, Y.; He, Y. H.; Guo, W.; Wang, Z. H. Observation of Gold Electrode Surface Response to the Adsorption and Oxidation of Thiocyanate in Acidic Electrolyte with Broadband Sum-Frequency Generation Spectroscopy. *Vib. Spectrosc.* **2016**, *85*, 122−127.
(69) Sengupta, S.; Moberg, D. R.; Paesani, F.; Tyrode, E. Neat Water-Vapor Interface: Proton Continuum and the Nonresonant Background. *J. Phys. Chem. Lett.* **2018**, *9* (23), 6744−6749.
(70) Gan, W.; Wu, D.; Zhang, Z.; Feng, R. R.; Wang, H. F. Polarization and Experimental Configuration Analyses of Sum Frequency Generation Vibrational Spectra, Structure, and Orientational Motion of the Air/Water Interface. *J. Chem. Phys.* **2006**, *124* (11), 114705.
(71) Gaigeot, M. P.; Sprik, M.; Sulpizi, M. Oxide/Water Interfaces: How the Surface Chemistry Modifies Interfacial Water Properties. *J. Phys.: Condens. Matter* **2012**, *24* (12), 124106.
(72) DelloStritto, M.; Piontek, S. M.; Klein, M. L.; Borguet, E. Relating Interfacial Order to Sum Frequency Generation with Ab Initio Simulations of the Aqueous Al_2O_3(0001) and (1120) Interfaces. *J. Phys. Chem. C* **2018**, *122* (37), 21284−21294.
(73) Hu, J. W.; Li, J. F.; Ren, B.; Wu, D. Y.; Sun, S. G.; Tian, Z. Q. Palladium-Coated Gold Nanoparticles with a Controlled Shell Thickness Used as Surface-Enhanced Raman Scattering Substrate. *J. Phys. Chem. C* **2007**, *111* (3), 1105−1112.
(74) Fang, P. P.; Li, J. F.; Lin, X. D.; Anema, J. R.; Wu, D. Y.; Ren, B.; Tian, Z. Q. A SERS Study of Thiocyanate Adsorption on Au-Core Pd-Shell Nanoparticle Film Electrodes. *J. Electroanal. Chem.* **2012**, *665*, 70−75.
(75) Piontek, S. M.; Tuladhar, A.; Marshall, T.; Borguet, E. Monovalent and Divalent Cations at the α-Al_2O_3(0001)/Water Interface: How Cation Identity Affects Interfacial Ordering and Vibrational Dynamics. *J. Phys. Chem. C* **2019**, *123* (30), 18315−18324.
(76) Das, M. R.; Borah, J. M.; Kunz, W.; Ninham, B. W.; Mahiuddin, S. Ion Specificity of the Zeta Potential of α-Alumina, and of the Adsorption of p-Hydroxybenzoate at the α-Alumina-Water Interface. *J. Colloid Interface Sci.* **2010**, *344* (2), 482−491.
(77) Heuft, J. M.; Meijer, E. J. Density Functional Theory Based Molecular-Dynamics Study of Aqueous Chloride Solvation. *J. Chem. Phys.* **2003**, *119* (22), 11788−11791.
(78) Eftekhari-Bafrooei, A.; Borguet, E. Effect of Electric Fields on the Ultrafast Vibrational Relaxation of Water at a Charged Solid-Liquid Interface as Probed by Vibrational Sum Frequency Generation. *J. Phys. Chem. Lett.* **2011**, *2* (12), 1353−1358.
(79) Schlaich, A.; Knapp, E. W.; Netz, R. R. Water Dielectric Effects in Planar Confinement. *Phys. Rev. Lett.* **2016**, *117* (4), 048001.
(80) Sverjensky, D. A. Prediction of Surface Charge on Oxides in Salt Solutions: Revisions for 1:1 (M+L-) Electrolytes. *Geochim. Cosmochim. Acta* **2005**, *69* (2), 225−257.

https://dx.doi.org/10.1021/jacs.0c01366
J. Am. Chem. Soc. 2020, 142, 12096−12105